NATIONAL AERONAUTICS
AND SPACE ADMINISTRATION

Research Grant NsG-306-63

The Design and Development of Rogowski Coil Probes for Measurement of Current Density Distribution in a Plasma Pinch

NsG-306

Report No. 740

Prepared by: Edward S. Wright
Assistant in Research

Approved by: Robert G. Jahn
Associate Professor
and Research Leader

and: Woldemar F. von Jaskowsky
Research Engineer

June 1965

Guggenheim Laboratories for the Aerospace Propulsion Sciences
Department of Aerospace and Mechanical Sciences
Princeton University
Princeton, New Jersey

ABSTRACT

32035

Small toroidal Rogowski coil probes have been constructed to measure directly the current density distributions in a large-radius plasma pinch discharge. When properly constructed, the EMF induced in these coils is proportional to the current passing through the center hole of the toroid, irrespective of the details of its distribution. Current density distributions determined by these probes in discharges at various pressures in two different pinch chambers are found to coincide well with the results of detailed magnetic probe mapping over the major portions of the profiles. In particular, current rise and position of current maxima are practically identical, whereas greater variance is noted in current sheet widths, and in measurements close to the chamber wall. On the basis of these results, further use of the Rogowski coil probe for plasma diagnostics seems indicated.

TABLE OF CONTENTS

LIST OF FIGURES

I. INTRODUCTION

Among the various possible diagnostic studies of self-field pulsed plasma gas accelerators, measurements of the interior current density distributions are perhaps the most infomative. The standard technique for determining these current distributions is by the use of magnetic probes inserted into the discharge chamber. The integrated output of the magnetic probe is proportional to the magnetic field at its location so that a series of magnetic probe readings at various locations when suitably plotted provides a determination of the magnetic field. Current density distributions may then be determined from the magnetic field by a series of simple arithmetical calculations whose exact form depends on the discharge geometry. For example, in the cylindrical pinch discharge, these calculations require finding $B_\theta r$ at two values of r and dividing their difference by the product of the change in r and the average r, to yield an approximation for $\mu_o j_z$, where B_θ is the magnetic field in the θ direction, r is the radial position from the center, μ_o is the permeability constant, and j_z is the current density in the z direction. It would be desirable if an accurate, reliable, and durable device existed which could measure current densities at any point in the discharge directly without the need for the more extensive data reduction required to find current densities from magnetic fields. The development of such a device based on the Rogowski coil principle was the goal of this investigation.

The basic measurement made by a Rogowski coil is of the rate of change of magnetic flux interior to the windings of an induction coil enclosing an area.[1,2] The EMF induced is electronically integrated, displayed and photographed on an oscilloscope, to yield direct temporal resolution of current enclosed by the coil in accordance with Maxwell's equations. A simple cross plot may then be made directly from the photographs to yield a spatial resolution of current density versus radius at the various times required for most diagnostic work.

All probe surveys and tests were undertaken in the 5" and 8" diameter cylindrical pinch chambers of the Electric Propulsion Laboratory, Guggenheim Laboratories, Princeton University, described in detail by Jahn et al.[3,4] elsewhere.

II. THEORY

A. Ampere's Law

The theory of the Rogowski coil is embodied in Maxwell's equations in the form of Ampere's and Faraday's Laws. Ampere's Law describes the sources of the curl of the magnetic field as the current density and the displacement current as follows:

$$\nabla \times \vec{B} = \mu_o(\vec{j} + \frac{d\vec{D}}{dt}) \qquad (1)$$

where $\vec{B}$ is the magnetic induction, $\vec{j}$ is the current density, $\frac{d\vec{D}}{dt}$ is the displacement current.

Consider Stokes' theorem in the form which relates the integral around any closed path of a vector field to the surface integral of the normal component of the curl of the vector taken over any surface which has the closed loop as its periphery.

$$\oint_{\Gamma} \vec{B} \cdot \vec{ds} = \int_S (\nabla \times \vec{B}) \cdot \vec{n}\, dS \qquad (2)$$

Substituting for curl $\vec{B}$ from (1) above, and neglecting the displacement current, we have:

$$\oint_{\Gamma} \vec{B} \cdot \vec{ds} = \mu_o \int_S \vec{j} \cdot \vec{n} \, dS \qquad (3)$$

And since the integral over $\vec{j}$ is the total current I through the surface S, we may write:

$$\oint_{\Gamma} \vec{B} \cdot \vec{ds} = \mu_o I \qquad (4)$$

Thus we see that the measurement of $\oint \vec{B} \cdot \vec{ds}$ around the closed curve Γ will provide us with a measurement of the current enclosed by Γ , irrespective of its distribution through S.

B. <u>Faraday's Law</u>

The necessary determination of $\oint \vec{B} \cdot \vec{ds}$ is provided by the Faraday's Law:

$$\nabla \times \vec{E} = - \frac{\partial B}{\partial t} \qquad (5)$$

Combining Stokes' theorem with Faraday's Law we have:

$$\oint_{\Gamma} \vec{E} \cdot \vec{ds} = \int_S (\nabla \times \vec{E}) \, \vec{n} \, dS = - \frac{\partial}{\partial t} \int_S \vec{B} \cdot \vec{n} \, dS \qquad (6)$$

By the customary definitions of flux ϕ and EMF, we have:

$$\phi \equiv \int_S \vec{B} \cdot \vec{n} \, dS \qquad (7)$$

$$\text{EMF} \equiv \oint_{\Gamma} \vec{E} \cdot \vec{ds} \qquad (8)$$

and therefore:

$$\text{EMF} = - \frac{\partial}{\partial t} \phi \qquad (9)$$

The final statement is the familiar result that the EMF around a loop of wire is equal to the rate of change of magnetic flux through the loop. Integration of (9) will now provide us with the measurement of B required to evaluate $\oint \vec{B} \cdot \vec{ds}$.

C. The Rogowski Coil

We must now design an instrument which will physically produce the desired response. The instrument consists of an induction coil of many turns bent into a circular shape corresponding to the closed curve Γ of equation (4). An EMF will be induced in the coil as a result of the current passing through the area enclosed by the induction coil which corresponds to the surface S of equation (3). The instrument is called a Rogowski coil and when suitably insulated and vacuum sealed so that it may be immersed in the plasma of a discharge, it becomes a Rogowski coil probe (see Figure 1). The performance of the Rogowski coil can be examined if we replace the integrals in equations (4) and (8) with finite sums.[5]

We designate the induced EMF (coil voltage) as u_i and get from (9):

$$\mathrm{EMF} = u_i = 10^{-8} F \sum_{v=1}^{n} \frac{dB_v}{dt} \qquad (10)$$

where F is the constant cross sectional area in cm^2 enclosed by each of the n evenly spaced turns of a long coil and B_v is the component of the magnetic field normal to the vth turn

If all the areas encircled by the turns are oriented perpendicular to the curve Γ, then B_v is always parallel to Δs, where Δs represents the distance between turns. If we take Δs to be sufficiently small, we can now approximate the integral in equation (4) by the sum:

$$\Delta s \sum_{v=1}^{n} B_v = 0.4 \pi I \qquad (11)$$

where I is the current in amperes enclosed by the closed coil.

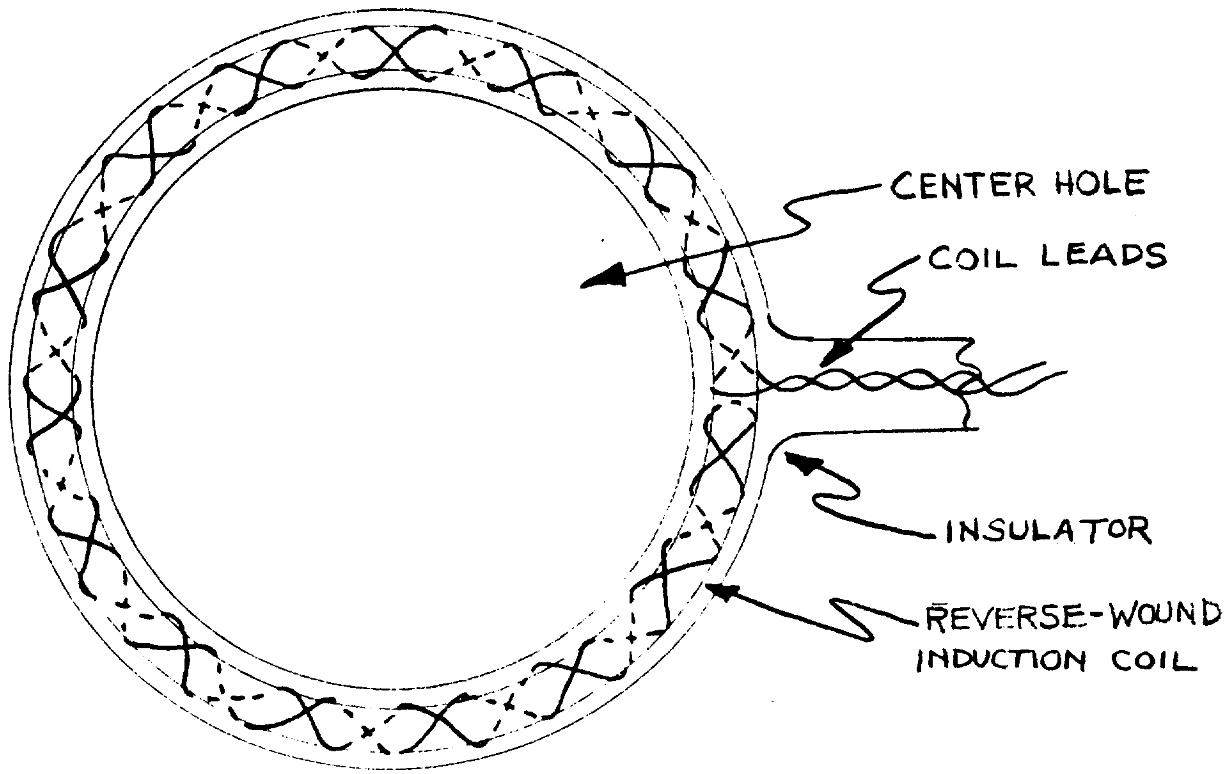

FIG 1a SCHEMATIC ROGOWSKI COIL

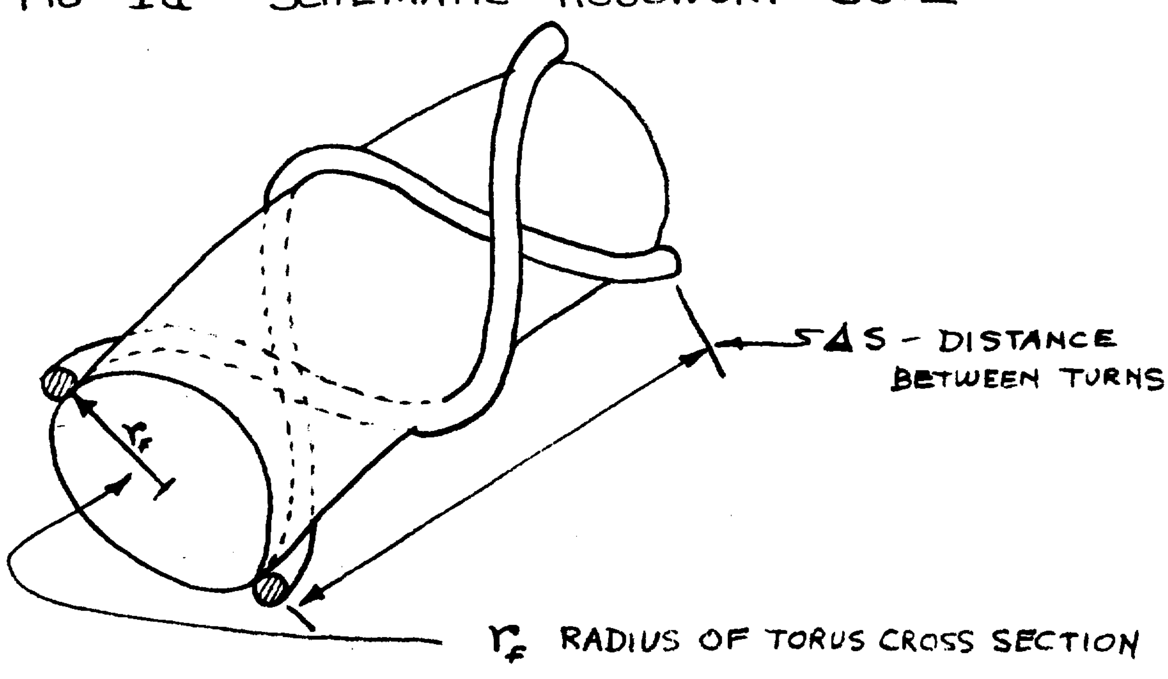

FIG 1b SECTION OF INDUCTION COIL

We now choose Δs to be constant and equal to ℓ/n where ℓ is the length of the coil in cm. and multiply both sides of (11) by F to get:

$$F \sum_{\nu=1}^{m} B_\nu = 0.4\,\pi\, I\, \frac{nF}{\ell} \tag{12}$$

Differentiating with respect to time yields:

$$F \sum_{\nu=1}^{m} \frac{dB_\nu}{dt} = \frac{0.4\,\pi\, nF}{\ell}\,\frac{dI}{dt} \tag{13}$$

Substitute (13) in (10) to get:

$$u_i = 0.4\,\pi \times 10^{-8}\,\frac{nF}{\ell}\,\frac{dI}{dt} \tag{14}$$

If we now integrate with respect to time, we get the final equations for the Rogowski coil relating the integrated coil signal to the current enclosed by the coil.

$$\int u_i\, dt = 0.4\,\pi \times 10^{-8}\,\frac{nF}{\ell}\, I \tag{15}$$

or

$$\int u_i\, dt = M\, I \tag{16}$$

where M, defined as the mutual inductance, is equal to $0.4\,\pi\,\frac{nF}{\ell} \times 10^{-8}$ and is a function of coil geometry only.

In summary then, the Rogowski coil measures the current it encloses provided that we use a large number of evenly spaced turns wound on a constant cross sectional area. Note that this result does not depend on any assumed symmetry for the distribution of the enclosed current.

III. CIRCUITS

Lumping all circuit elements and neglecting stray capacitances and inductances, we may represent the measuring circuit as follows:[5]

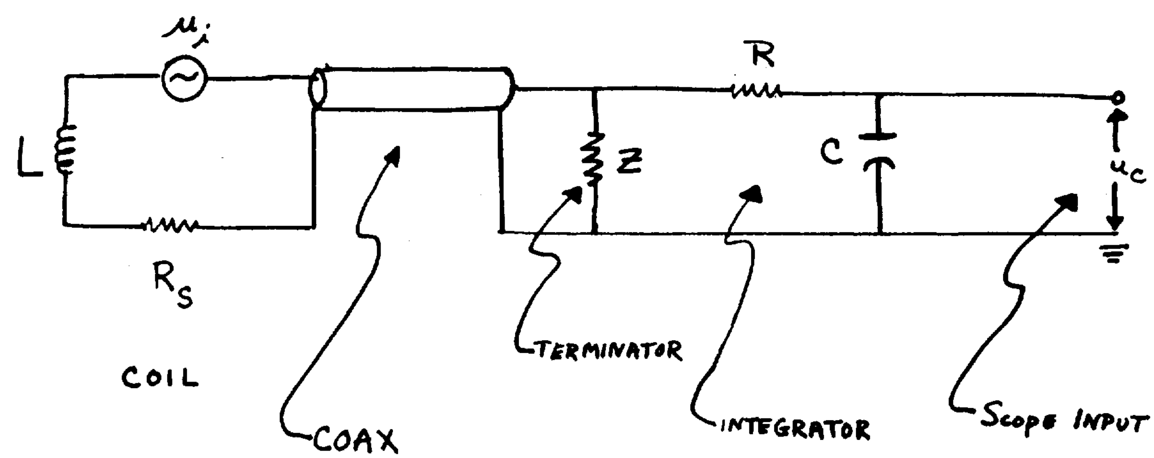

FIG 2 CIRCUIT DIAGRAM

The circuit equation is:

$$u_i = LC(1 + \frac{R}{Z}) \frac{d^2u_c}{dt^2} + [\frac{L}{Z} + RC + R_sC (1 + \frac{R}{Z})] \frac{du_c}{dt} + (1 + \frac{Rs}{Z}) u_c \qquad (17)$$

integrating and using equation (16), we get:

$$MI = LC(1 + \frac{R}{Z}) \frac{du_c}{dt} + [\frac{L}{Z} + RC + R_sC (1 + \frac{R}{Z})] u_c + (1 + \frac{Rs}{Z}) \int u_c dt \qquad (18)$$

Since we require that u_c be proportional to I, we must require that the first and third terms on the right hand side of (18) be negligibly small. These conditions are met provided:

$$LC(1 + \frac{R}{Z})\omega_o \ll \frac{L}{Z} + RC + R_sC\ (1 + \frac{R}{Z}) \qquad (19)$$

$$\frac{L}{Z} + RC + R_sC\ (1 + \frac{R}{C}) \gg \frac{1}{\omega_u}\ (1 + \frac{R_s}{Z}) \qquad (20)$$

where ω_o is the upper limiting frequency which can be read on the oscilloscope and ω_u is the lower limiting frequency used in this case as the ringing frequency of the discharge.

Typical values of the circuit components, coil, and discharge are as follows:

$L = 25 \times 10^{-9}$ Henries $\qquad \omega_o = \pi \times 10^{+7} \sec^{-1}$

$C = 1 \times 10^{-8}$ Farads $\qquad \omega_u = 2 \times 10^{5} \sec^{-1}$

$R = 2 \times 10^{3}$ Ohms

$Z = 10^{2}$ Ohms

$R_s = 3$ Ohms

For these values we have (approximately)

From (19) $\quad 1.5 \times 10^{-7} \ll 2 \times 10^{-5}$

From (20) $\quad 6 \times 10^{+3} \gg 5 \times 10^{-6}$

so that the conditions required for the circuit are met.

IV. DESIGN AND CONSTRUCTION

A. Criteria

The following criteria are established for the Rogowski coil probe:

1. Signal strength: Signal strength on the order of 1 volt unintegrated is required since noise effects would become dominant at lesser values. This value is estimated from equation (14) $u_i = 0.4\pi \times 10^{-8} \frac{nF}{\ell} \frac{dI}{dt}$.

2. Inductance: Self inductance of the coil must be kept to a minimum as can be inferred from equation (19). Self inductance may be estimated by the long coil formula[5]

$$L = \frac{0.4 \pi F n^2 \times 10^{-8}}{\ell} \text{ henries} \tag{21}$$

Note that although signal strength increases with the number of turns, inductance increases as the square of the number of turns so that it is unwise to attempt to increase signal strength to higher values by the addition of an indefinite number of turns.

3. Discharge distortion: It is obvious that the presence of the probe must produce some physical distortion of the discharge. While we cannot be sure of this perturbation, it appears to be reasonable to insist that the annular cross-sectional area of the induction coil and its insulation be several times less than the area enclosed by the coil, thus minimizing squeeze of the plasma into the hole or exclusion from it. On the other hand, the hole should be smaller than the width of a typical current sheet which we wish to examine.

4. Other criteria: The probe should be relatively easy to construct, easy to use, and durable, or the advantage of its use as compared to reduction of magnetic probe data becomes doubtful.

B. Construction of Probe

Two general types of probe were constructed. The "doped" probe had a rigid coil doped with successive layers of Glyptal and epoxy for insulation while the "shepherd's crook" probe used a glass insulator in the form of a hollow shepherd's crook into which a coil wound on a flexible core was inserted.

The former has the advantages of less bulk for a given signal strength and possibly greater geometric symmetry, but was discarded in favor of the latter because of the non-uniformity and lack of durability of the doped insulation. Figure 3 shows some of the early attempts of probe construction. Figures 4 and 5 show the design found most closely to satisfy the criteria, and Figure 6 demonstrates the construction of the induction coil. The glass insulator was fabricated by the "B" site shop of the Plasma Physics Laboratory, Forrestal Research Center. Figure 7 gives some of the design parameters of the successful shepherd's crook probe.

Once a design of the probe has been decided, the single most important technique to observe in its construction is meticulously to avoid the inadvertant introduction of any spurious loops which will read flux changes at undesired locations. Loops at terminations, in the leads, or in the coil itself are difficult to avoid and lead inexorably to distortions.

C. <u>External Currents</u>

Rogowski coils are customarily employed where they enclose the entire current to be measured.[1,2,5,6] In other words, there are no significant currents external to the area enclosed by the induction coil. However, for the application here considered, by far the greater portion of the current of the circuit will be exterior to the opening of the probe so that it becomes essential to consider the effects that external currents have on the response of the probe. $\oint \vec{B} \cdot d\vec{s}$ around the curve Γ due to currents external to Γ must be zero since the sources are not enclosed by Γ (conservative field). The mechanism by which the coil physically conforms to this requirement is by the cancellation of signals generated by opposite portions of the coil. It is essential that this

AP25-P27-65

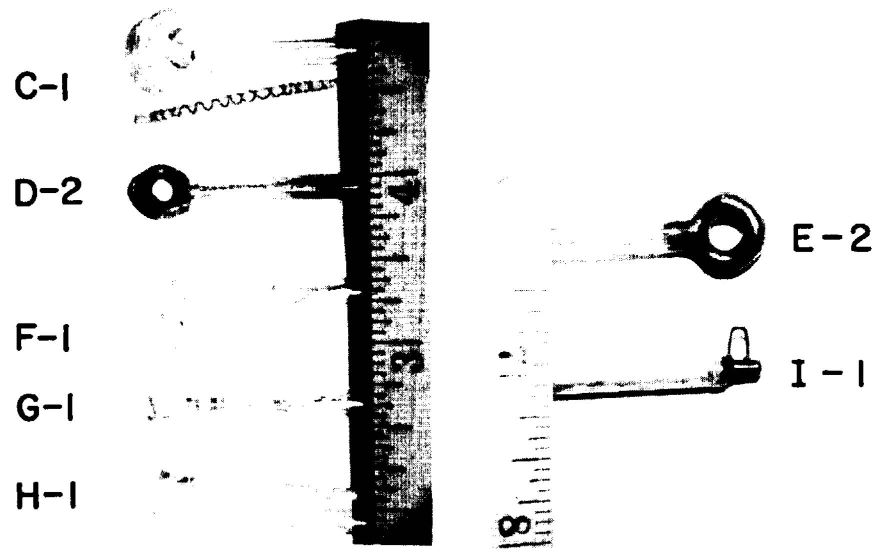

EARLY TYPES OF PROBES

FIGURE 11

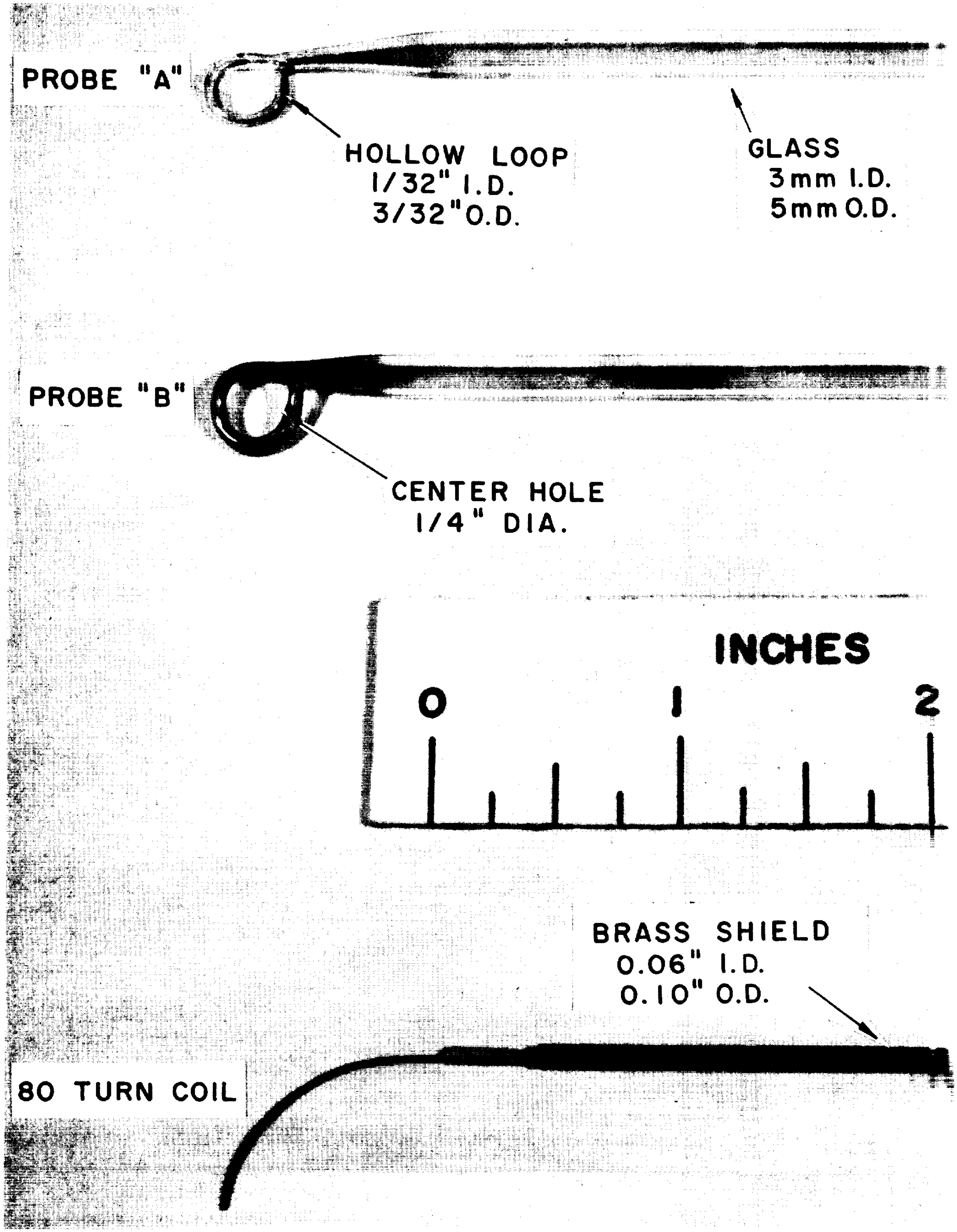

SHEPHERD'S CROOK PROBE & INDUCTION COIL INSERT

FIGURE

MP25-P24-65

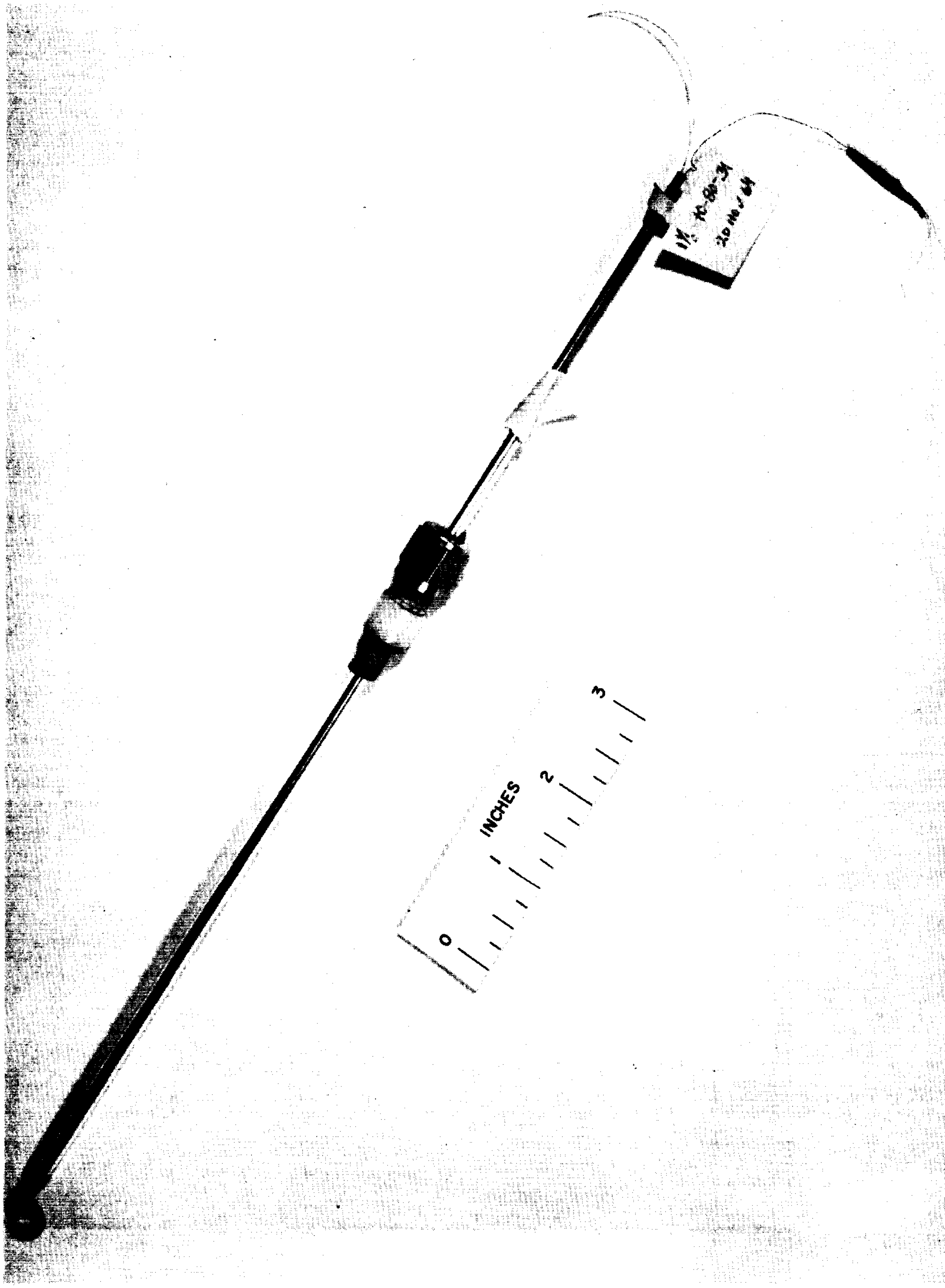

FIGURE 13

AP25-P25-65

AP25-P26-65

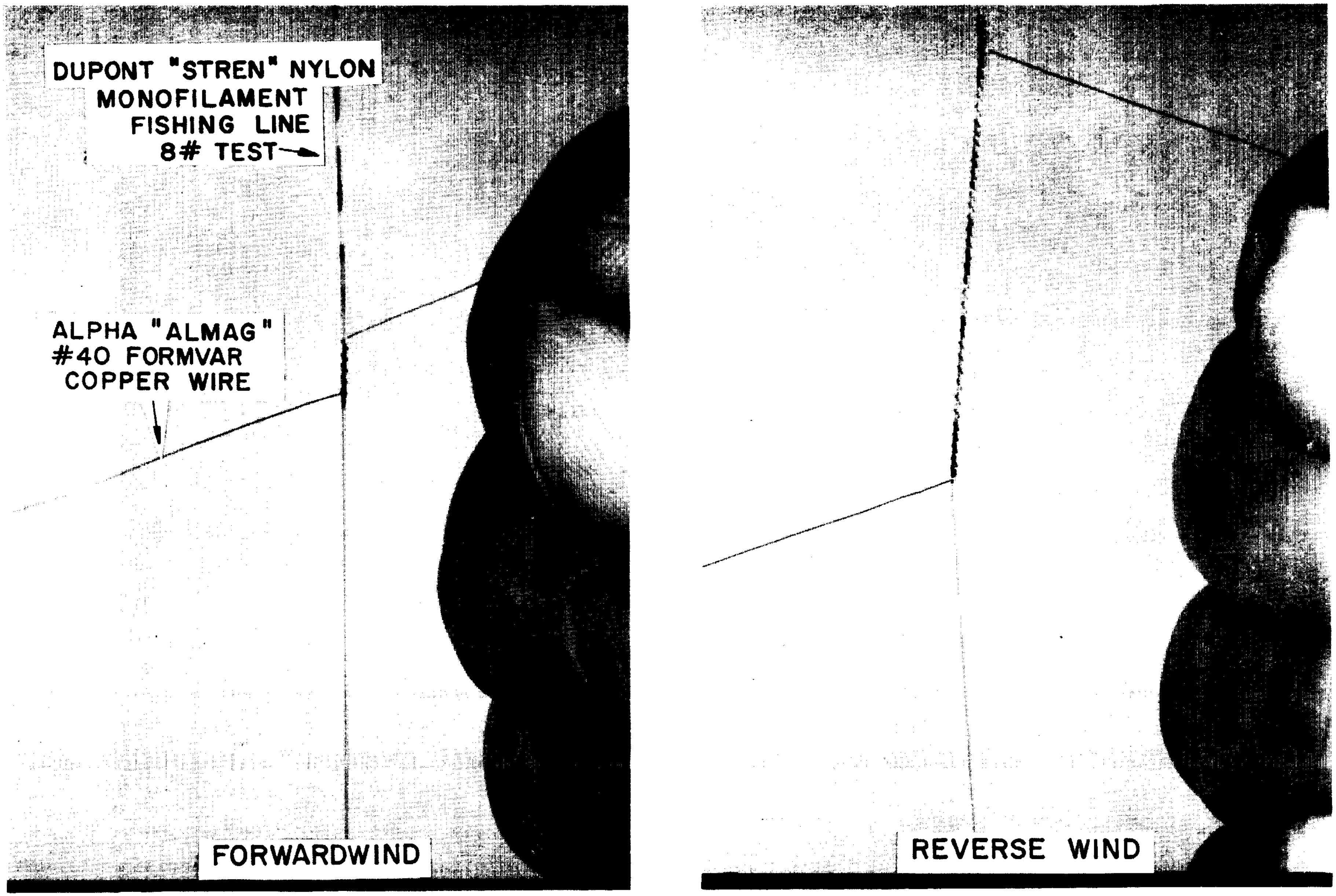

FIGURE

WINDING OF INDUCTION COIL

Typical Coil Design

winding wire	#40 Formvar
turns (n)	105
radius of core (r_f)	.015 cm
cross sectional area of coil $F = \pi r_f^2$	6×10^{-4} cm^2
length of coil ℓ	3 cm
(j) max estimated	4×10^{9} $\frac{\text{amp}}{\text{cm}^2\text{sec}}$
area enclosed A (for typical shepherd's crook probe)	0.3 cm^2
estimated u_{imax} = $\frac{0.4 \pi F n A(j)max \times 10^{-8}}{\ell}$	0.3 volts
calculated inductance $L = \frac{0.4 \pi F n^2 \times 10^{-8}}{\ell}$	25×10^{-9} H

FIG. 7

cancellation take place to a high degree in our attempt to adapt the Rogowski coil for use in the interior of the pinch device.

If for some reason the coil is not symmetric in the sense that it does not form a closed curve, or that the turns are not evenly spaced, or the areas enclosed by the coil windings vary, it is seen that large errors can be expected when the voltages induced by the flux changes due to external currents are not cancelled.

Actually, the current distribution in the pinch gives rise to a $\vec{B}$ field which is overwhelmingly in the θ direction. Since the finite thickness of glass at the end of a shepherd's crook probe prevents us from realizing a completely closed curve, it becomes necessary to orient this gap so that it causes the least signal distortion due to lack of cancellation of emf from external currents (see Figure 8). For example, early probes of the shepherd's crook design constructed with the gap parallel to θ acted in fact as "negative" magnetic probes and gave essentially $\vec{B}$ field readings rather than current densities since the signals received at the opposite side of the gap due to external currents were not cancelled and this distortion was the dominant EMF induced. Corrections were made in later models by overlapping the probe so that the gap appeared in the Z direction. Another possible solution would be to place the gap parallel to the r direction.

V. TESTS

In addition to the current density versus radius surveys displayed in Figures 14 through 17, numerous other types of tests were conducted with the R coil probes to establish the validity of the obtained data.

1. Plugged hole. If the probe reads only current passing through the hole as designed, then a null reading

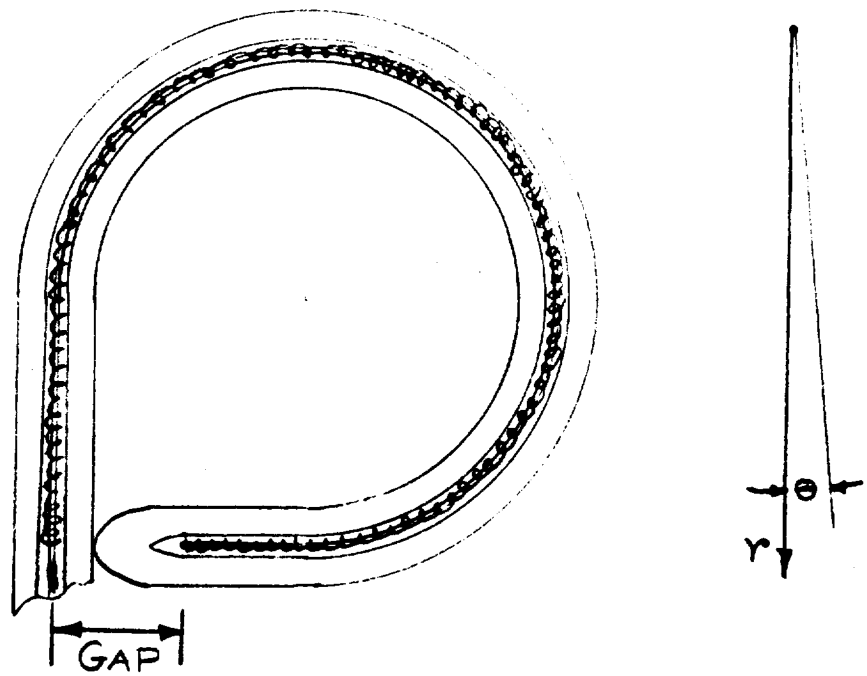

FIG 8a SHEPHERD'S CROOK PROBE WITH INDUCTION COIL GAP CAUSED BY GLASS THICKNESS

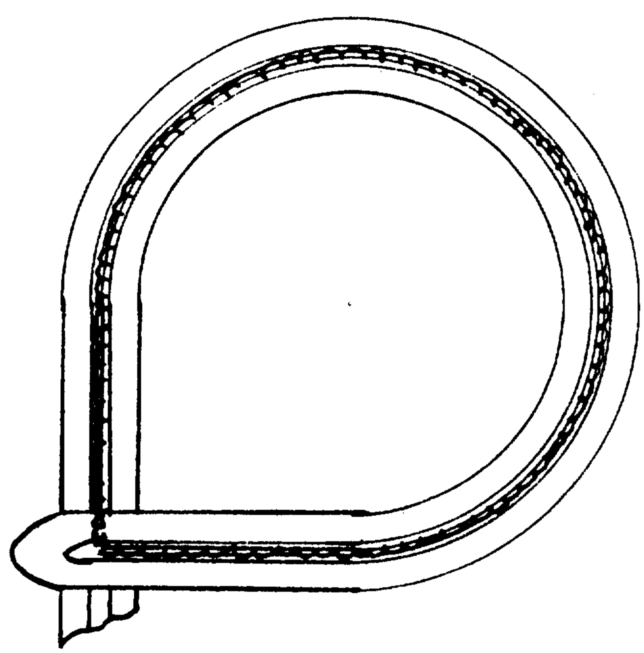

FIG 8b GAP ELIMINATED IN θ DIRECTION BY OVERLAPPING

should be obtained with the hole plugged. Plugs were fashioned of various materials, but the most satisfactory was found to be mylar sheet cemented in with Duco cement and thus readily removable with acetone solvent. Figure 9a displays typical results, showing amplitude reduced by approximately 80% for the first current sheet and 90% for the second current sheet.

2. Orientation. When the probe is inserted in the pinch chamber, it is possible to rotate the hole so that its axis is parallel to either Z or θ or anywhere in between. Since the current in the cylindrical pinch is primarily j_z, a near null signal should be obtained when the hole is oriented so that its axis lies along θ. This effect is displayed in Figure 9b. It is also observed that the results are relatively insensitive to rotations averaging 10 to 20 degrees from the normal position, indicating that orientation of the probe is not critical.

3. Shorting posts. Discharges in the pinch chamber at reduced voltage and capacitance with a shorting post installed between the electrodes provide certain tests dependent on the orientation of the probe with respect to the shorting post. For example, when the shorting post goes through the hole of the probe identical response to that of the main Rogowski coil reading total current in the pinch chamber is obtained as shown in Figure 10a. If the post is outside the hole of the probe, null signals should be obtained. Such results are shown in Figures 10b, 10c, and 10d. The almost complete null obtained when the probe is in the position shown in 10b is more significant than the discernible signal obtained when the probe is in position shown in 10d since, in an actual gas discharge, the $\vec{B}$ field due to all currents in the cylindrical configuration does not precede the currents on the inward pinch.

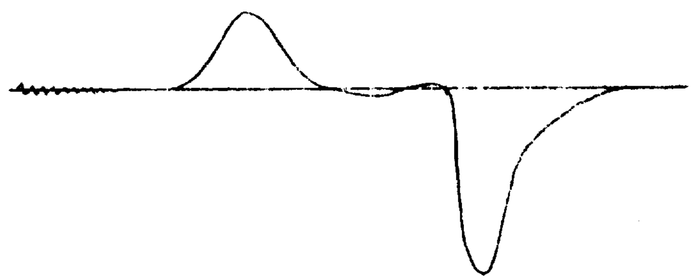

FIG 9a NORMAL SIGNAL A105 PROBE AT 3", 120 μ ARGON

FIG 9b A105 PROBE WITH CENTER HOLE PLUGGED

FIG 9c A105 PROBE ROTATED 90° WITH LOOP UP

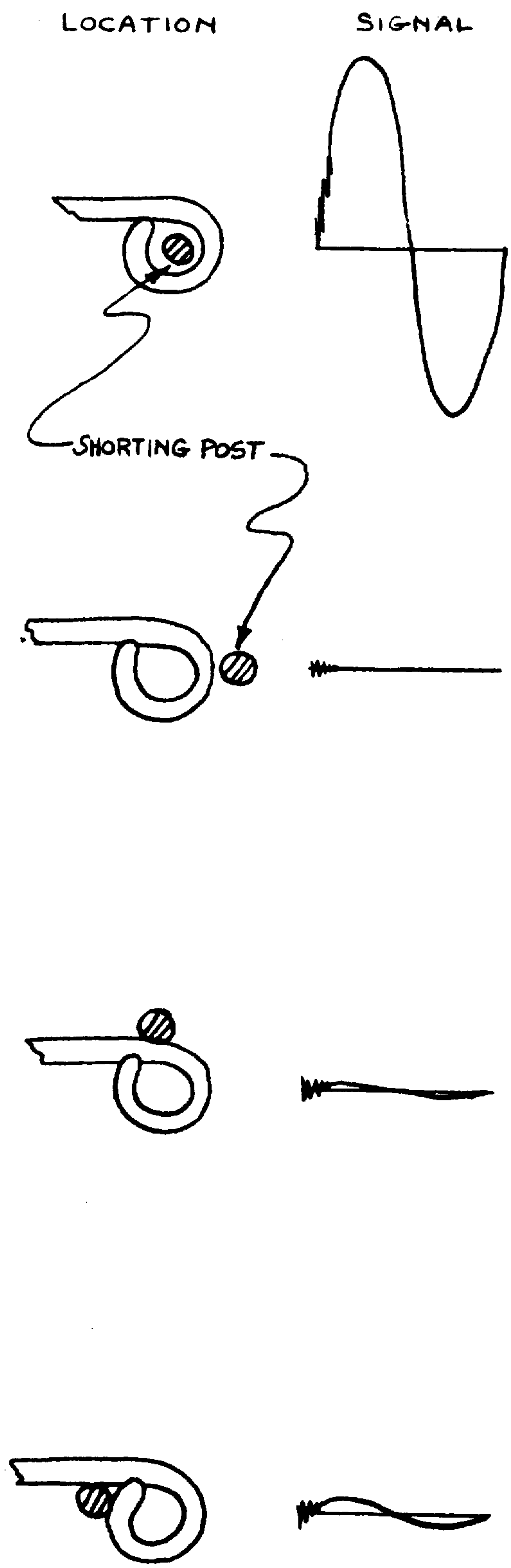

FIG 10a
SHORTING POST THROUGH CENTER HOLE

FIG 10b
SHORTING POST AT REAR

FIG 10c
SHORTING POST AT SIDE

FIG 10d
SHORTING POST AT FRONT

4. Farside. It is conceivable and, in fact, has been demonstrated by other experiments with magnetic probes at the Electric Propulsion Laboratory that the plasma may actually propagate down the glass tube at a faster rate than the main pinch propagates, leading to early time of arrival trajectories. In order to test this effect, tests were run with the probe extending more than halfway across the chamber so that the inward pinching current sheet impacted directly upon the probe. No significant differences were noted in the time of arrival, which can be ascribed to the fact that the R coil probe is offset so that the current sheet impacts on it directly in the standard position, even when a portion of the plasma might be preceding the main current sheet down the glass tube. Since farside surveys greatly increase the noise superimposed on the basic signal, none are included in this report.

5. Electrostatic. Originally all probes were tested for electrostatic pickup by various circuit alterations. For example, see Figure 11. It is now felt that a null signal received on the orientation test at 90° rotation provides a satisfactory electrostatic test since electrostatic pickup should be independent of coil orientation.

6. Reproducibility. Hundreds of different oscilloscope photos have established the reproducibility of results obtained with the miniature Rogowski coil probe. Typically, these photos show some variance in the amplitude and shape of the first current sheet, but display nearly identical response to the second and following current sheets as the pinch chamber discharges ring down. Since the first sheet propagates into a gas which is largely unionized, while the second sheet propagates into the unrelaxed completely ionized gas left by the first sheet, the probe response is felt to be consistent with the physical situation. Figures 12a and

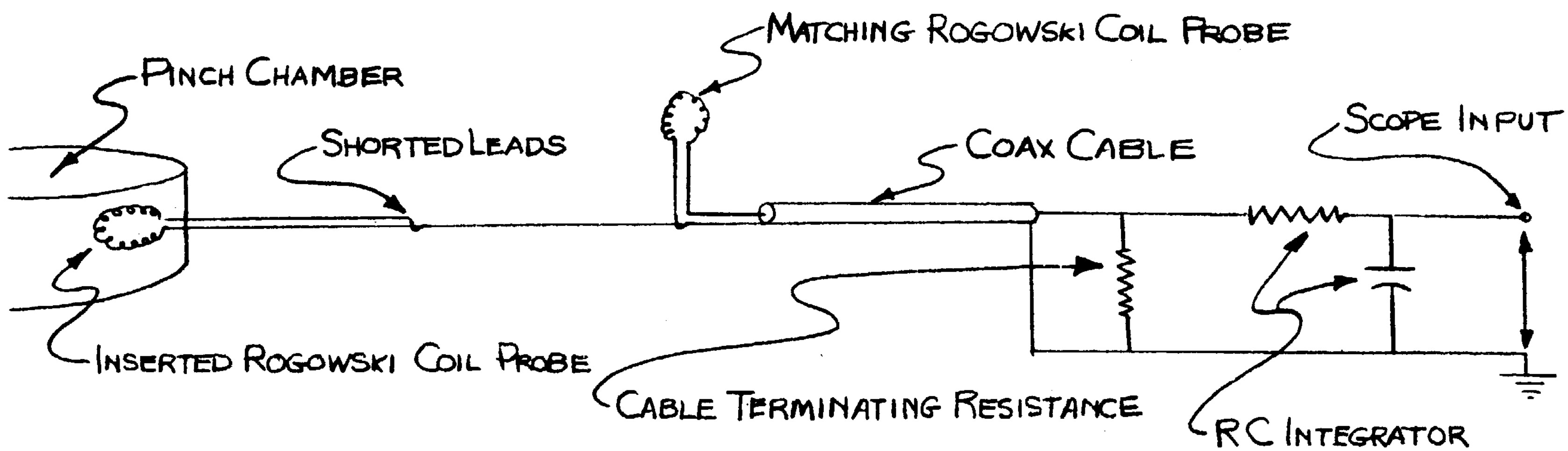

FIG 11 CIRCUIT DIAGRAM USED FOR EARLY ELECTROSTATIC TESTS

FIGURE 12 a

FIGURE 12 b

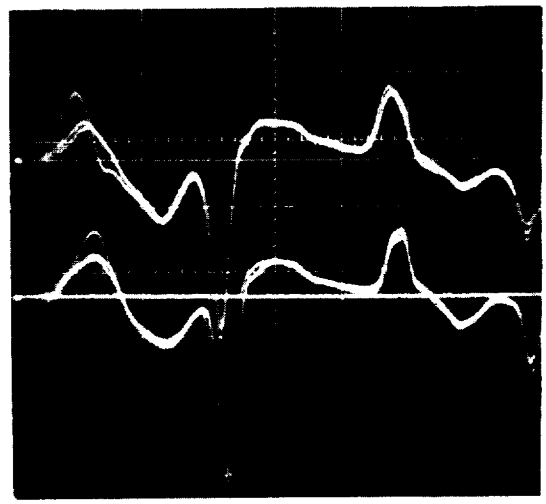

REPRODUCIBILITY OF PROBE RESPONSE

AP25 R 4031-65

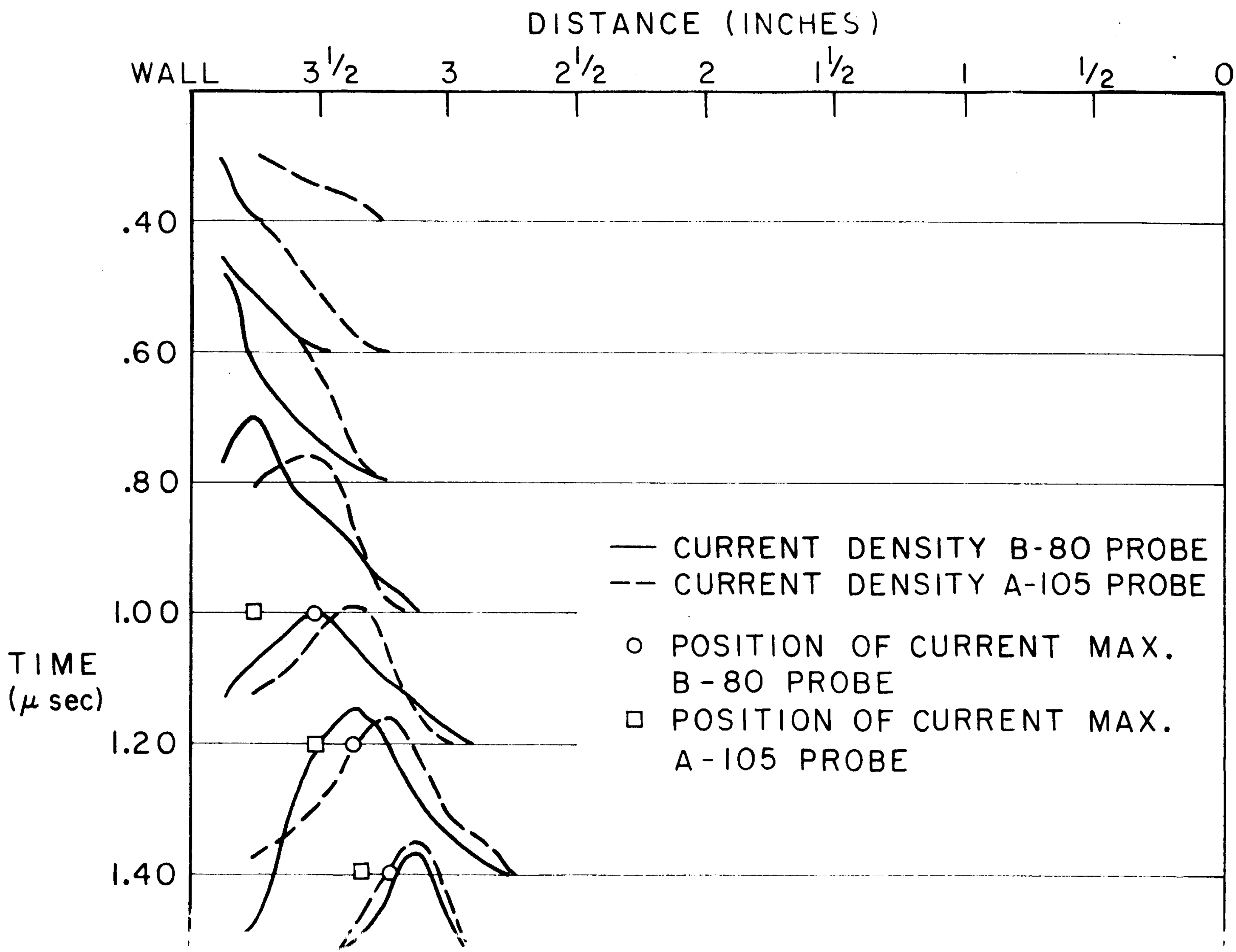

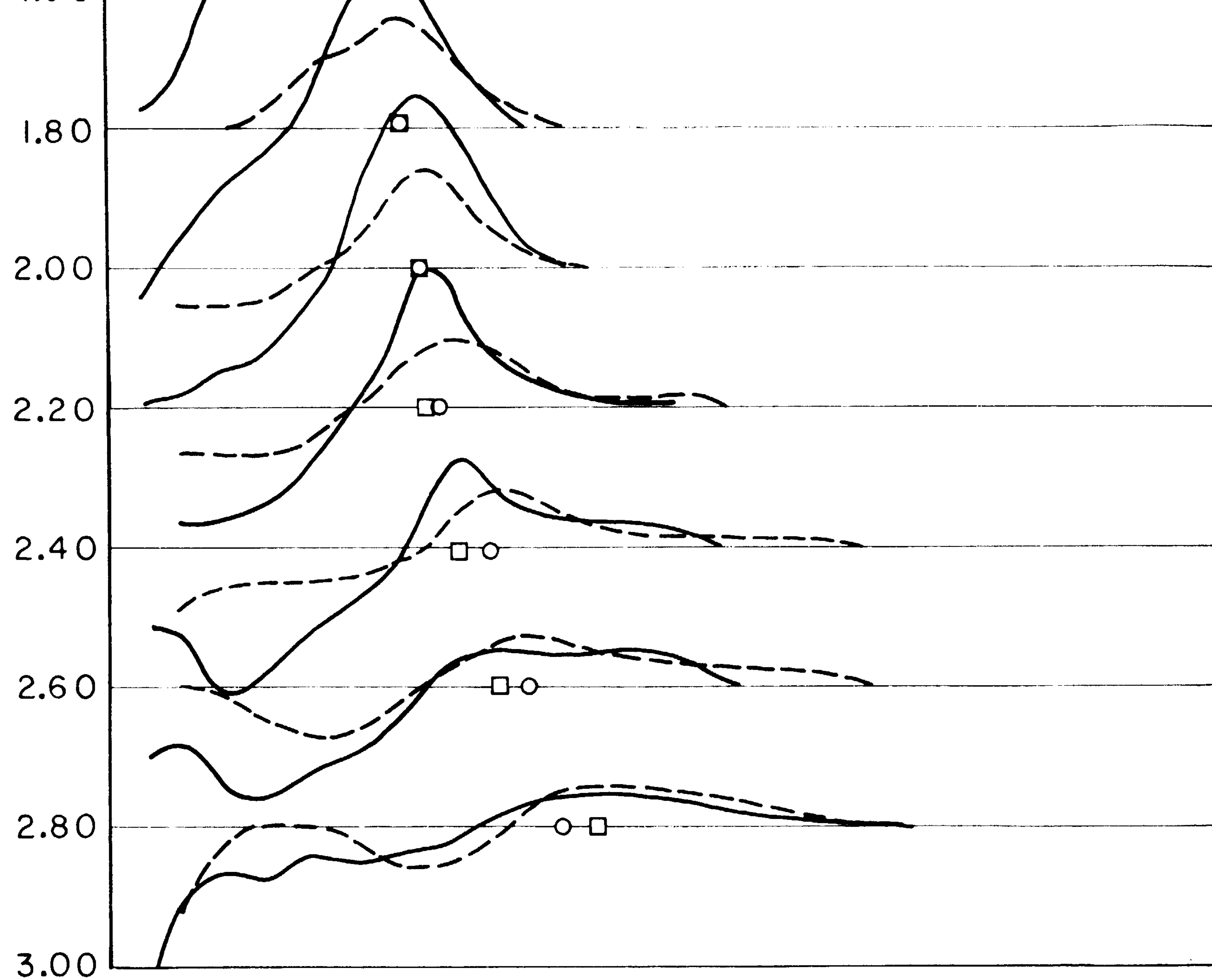

CURRENT DENSITY VS RADIUS FOR A-105 & B-80 PROBES AT 120 μ ARGON IN THE 8" CHAMBER

FIGURE 24

12b display typical results with variance of first sheet response, but uniform response for following sheets. The photo consists of three traces at each of two radial positions.

Reproducibility of results for different surveys conducted at different times with different probes are displayed in Figure 13. The variations which exist appear to be no more than would be realized in comparing two magnetic probe surveys with the exceptions as will be noted in VII.

VI. RESULTS

Current density distribution plots obtained with the Rogowski coil probes are presented in Figures 14, 15, 16, and 17. These figures are produced by directly cross plotting the current versus time photographs taken at the oscilloscope at various radial positions, into a current versus radius plot at various times. The first three surveys are from the 8" pinch chamber in argon at pressures of 30 μ, 120 μ and 480 μ respectively, while the last survey was made in the 5" pinch chamber at 120 μ of argon. These results are compared with data obtained previously by other researchers at the Electric Propulsion Laboratory in the same pinch chambers from magnetic probe data. It is seen that in general there is very close agreement between the two sets of results throughout most of the discharge. This implies that quantitative mapping of current density distribution with Rogowski coil probes is feasible.

Agreement is particularly good concerning current rise times and positions of current maxima after the first one-half microsecond of the discharge. For these considerations the two sets of data can be considered identical when the accuracy with which the oscilloscope photos may be read and the accuracy with which the probe is located are considered.

Larger discrepancies between the two types of survey may be noted in the shape of the current form after the current maximum has passed. Although this is not noticeable in the 30 μ, 8" chamber case (Figure 14) it does appear in the 120 μ case (Figures 15 and 17). This effect typically broadens the width of the current pulse as determined by the Rogowski coil survey.

In all cases, it will be noted that the Rogowski coil probe will not produce results closer to the wall than 1/4" to 1/8" simply because of its physical size as the radial position of the coil is determined by the position of the center of the central hole.

VII. ADVANTAGES AND LIMITATIONS

The obvious advantage of the Rogowski coil probe is the saving of time required to reduce magnetic probe data to current densities. In addition, it should be noted that data provided by the Rogowski coil probe is more reliable than magnetic probe data near the center of the pinch since reduction of probe data depends on $\frac{1}{r} \frac{\partial (Br)}{\partial r} = \mu_o j$ (ampere's law for the cylindrical pinch) and thus becomes increasingly inaccurate as r approaches zero. Conversely, the larger physical size of the Rogowski coil makes it less dependable for determination of current near walls as is shown in Figures 14 and 15. Also, greater discrepancies between data obtained by the two methods exist in the "tail" of the current sheet. This effect may be noted in Figure 15 and in Figure 13 which compare two Rogowski coil probes. This unreliability might possibly be due to trapping of plasma by the probe and since it has not been consistently eliminated, less reliance should be placed on current profiles obtained behind the current sheets.

AP 25 R 4029-65

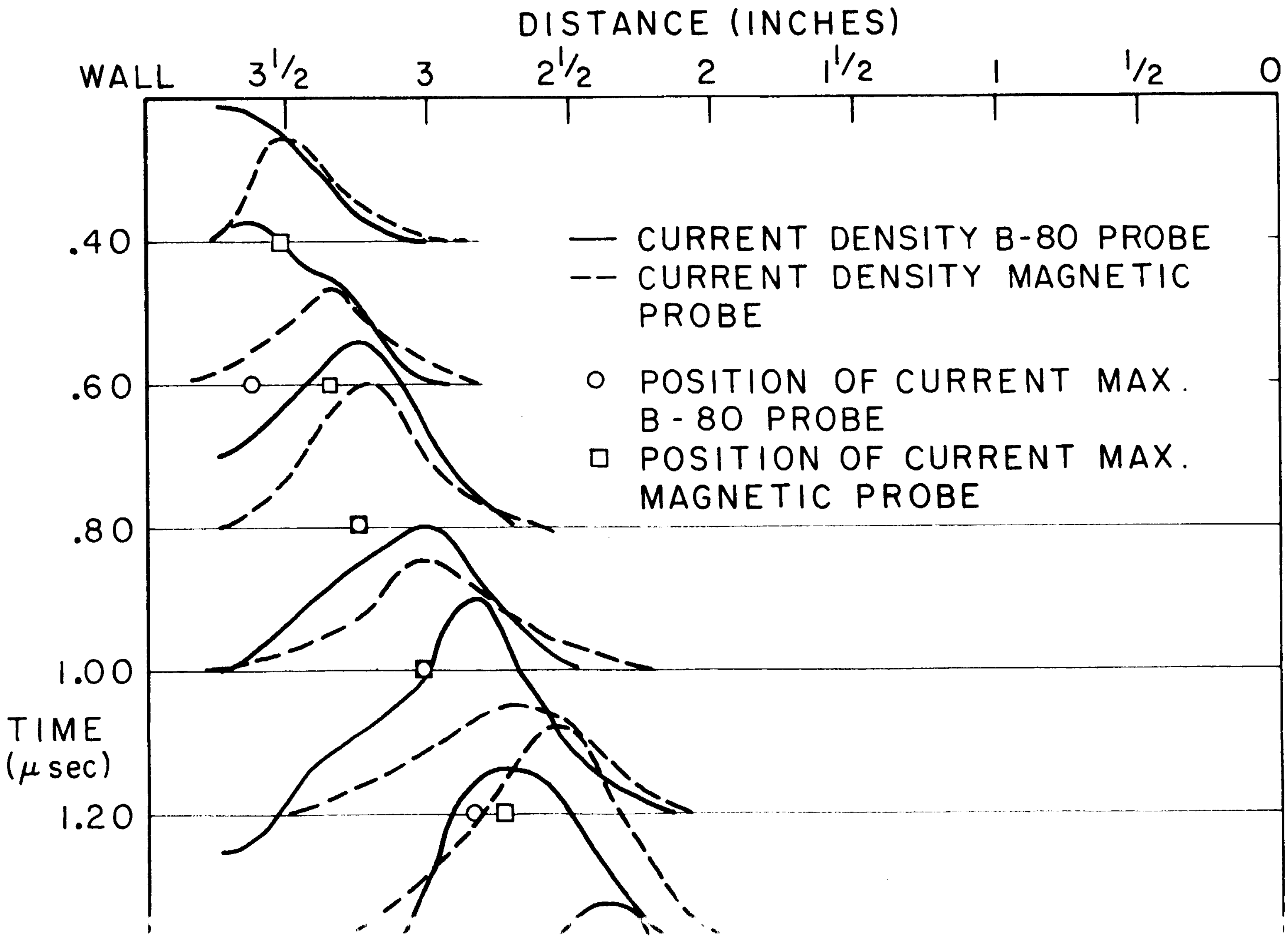

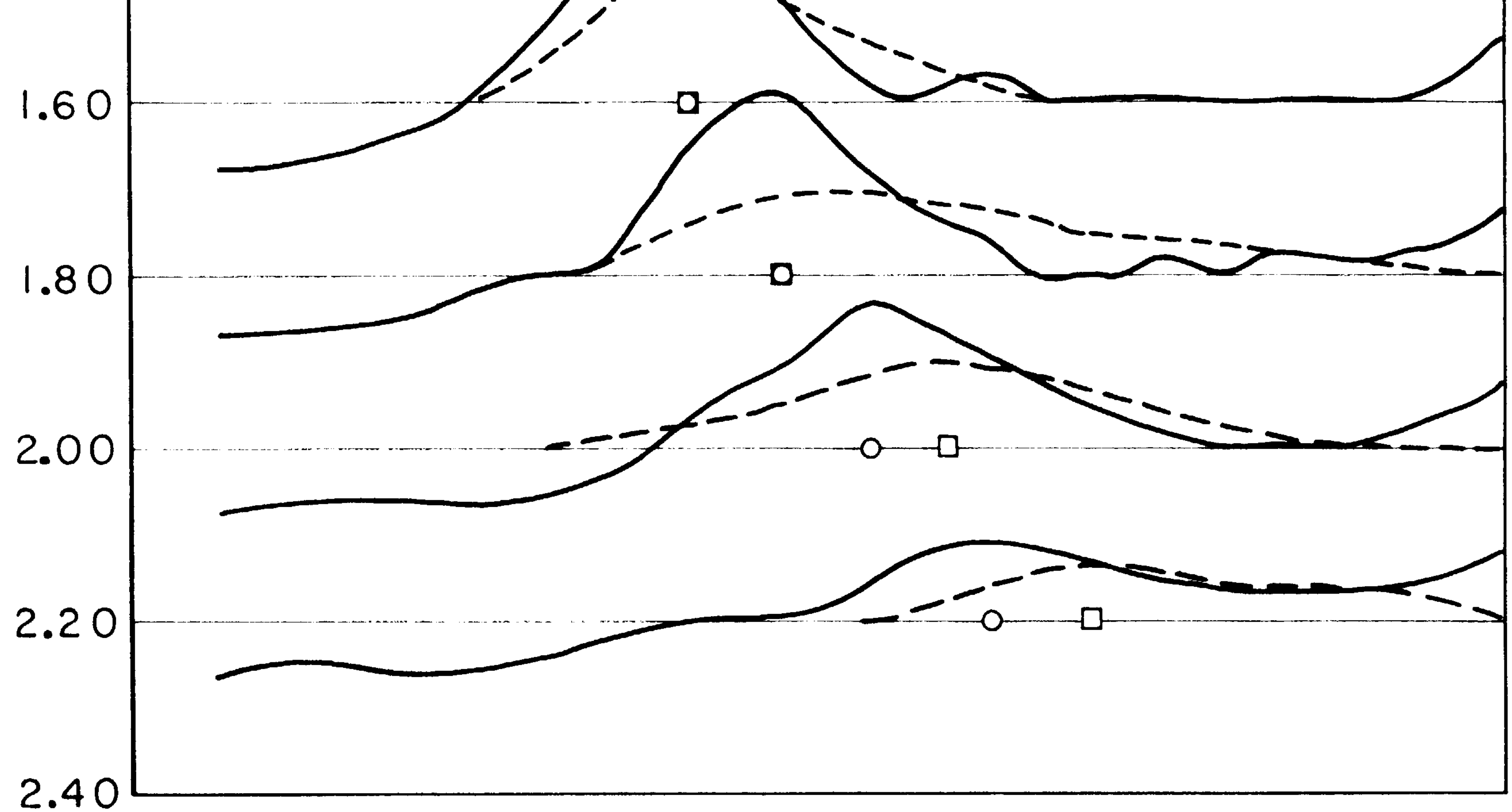

CURRENT DENSITY VS RADIUS FOR 30μ ARGON
IN 8" CHAMBER WITH B-80 ROGOWSKI COIL PROBE

FIGURE

N° 25 R 4028-65

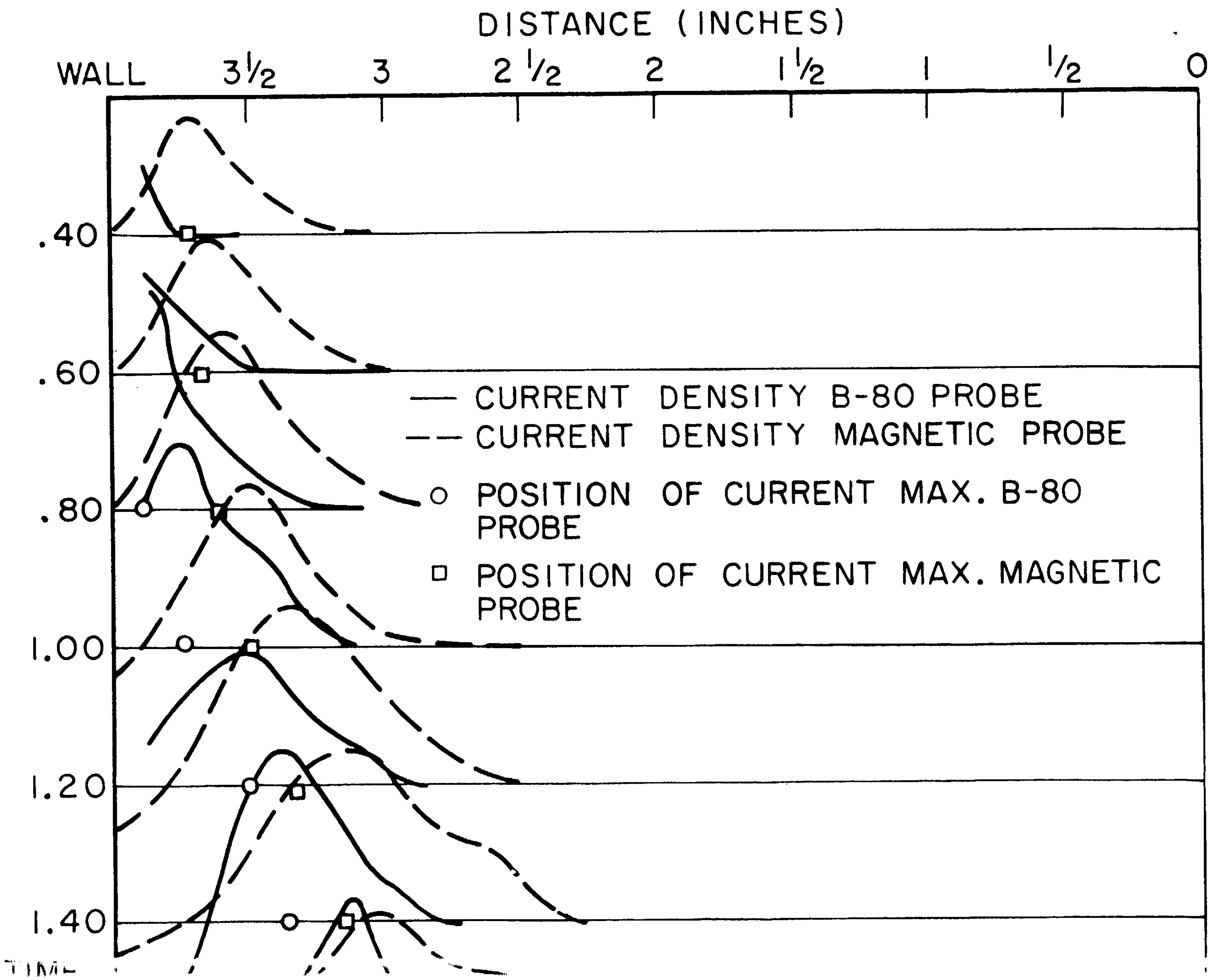

DISTANCE (INCHES)
WALL
3 1/2
3
2 1/2
2
1 1/2
1
1/2
0
.40
.60
.80
1.00
1.20
1.40
TIME
— CURRENT DENSITY B-80 PROBE
-- CURRENT DENSITY MAGNETIC PROBE
○ POSITION OF CURRENT MAX. B-80 PROBE
□ POSITION OF CURRENT MAX. MAGNETIC PROBE

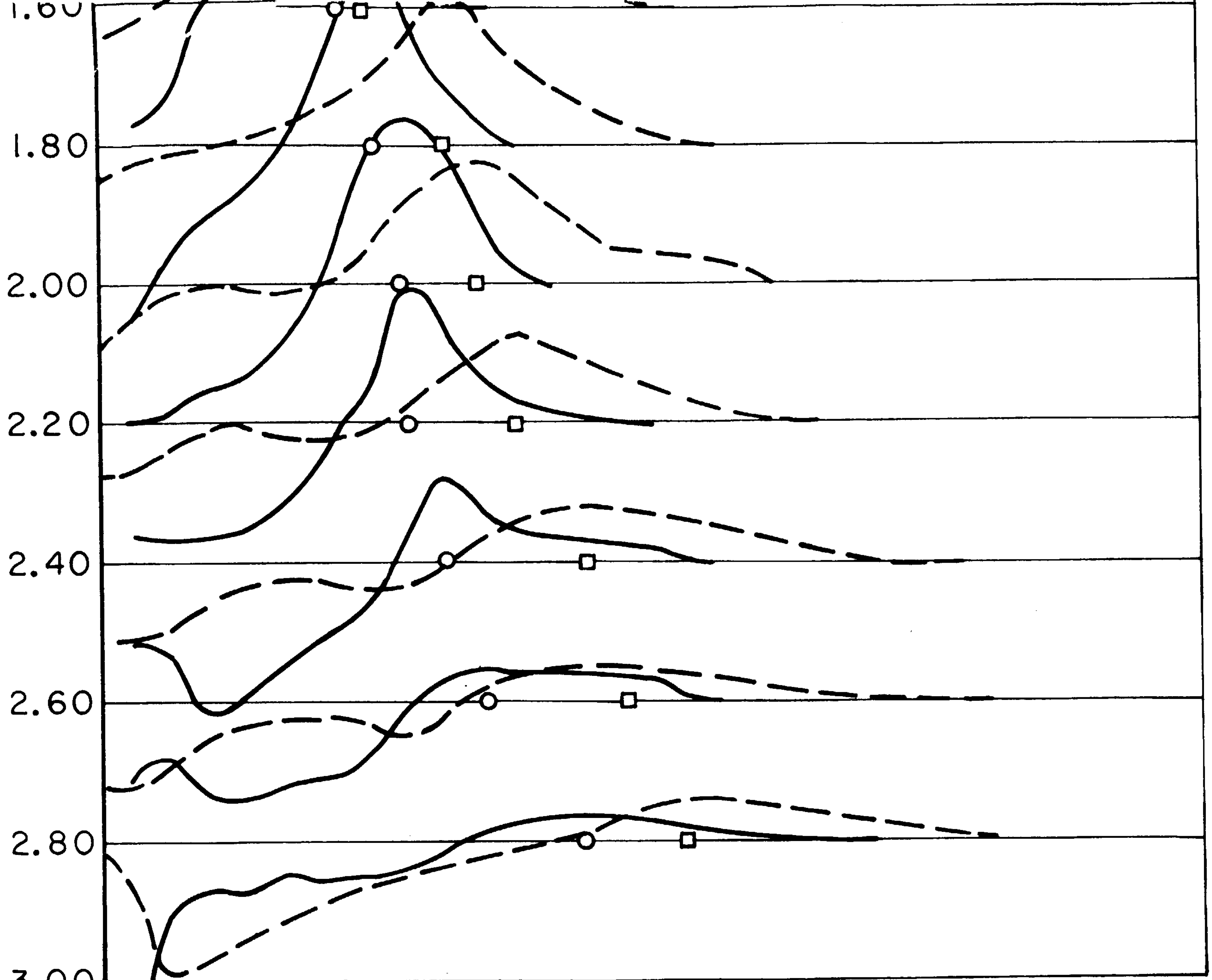

CURRENT DENSITY vs RADIUS FOR 120μ ARGON IN 8"
CHAMBER WITH B-80 ROGOWSKI COIL PROBE

FIGURE

AP25 R 4082-..

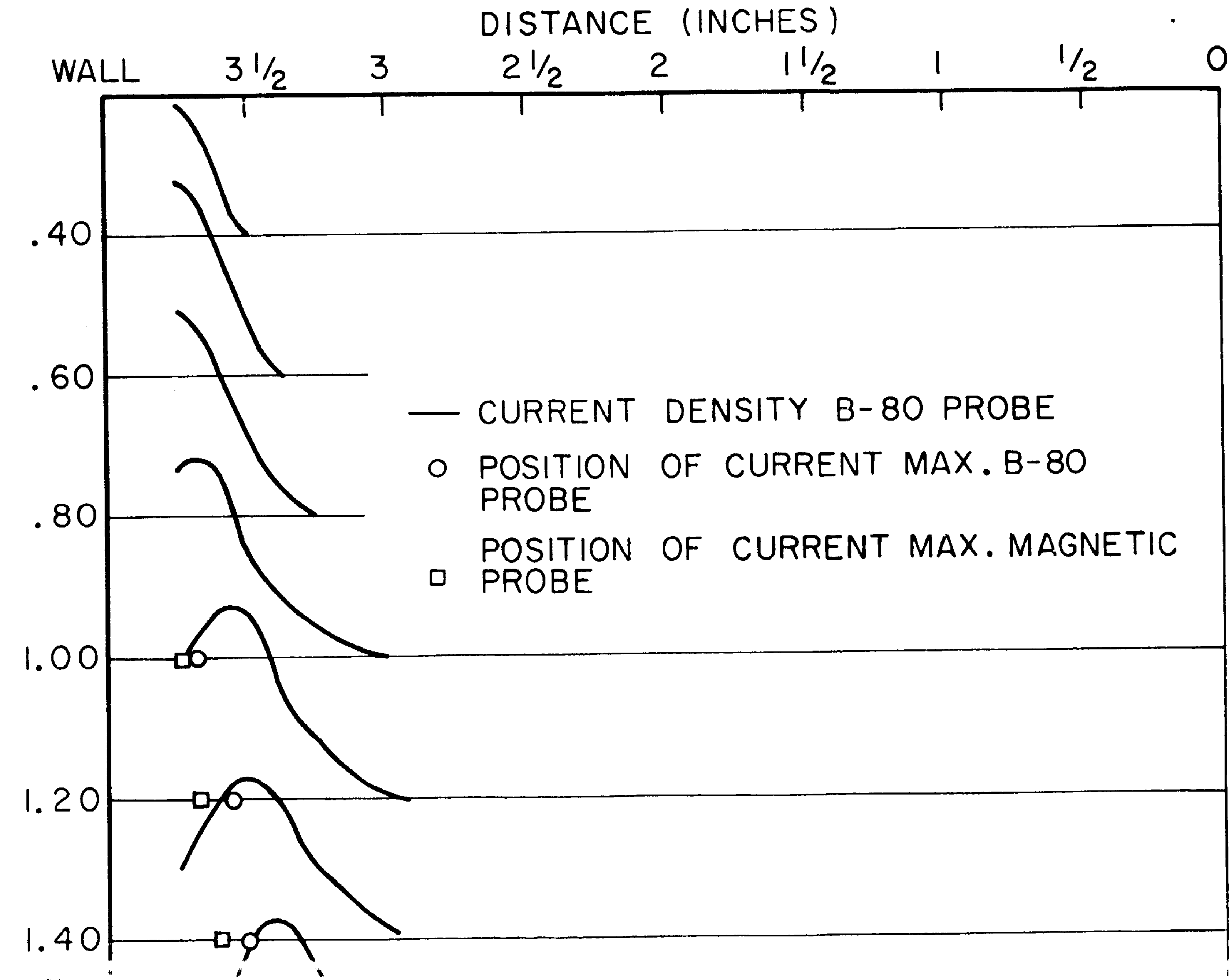
DISTANCE (INCHES)
WALL
3 1/2
3
2 1/2
2
1 1/2
1
1/2
0
.40
.60
.80
1.00
1.20
1.40
— CURRENT DENSITY B-80 PROBE
○ POSITION OF CURRENT MAX. B-80 PROBE
□ POSITION OF CURRENT MAX. MAGNETIC PROBE

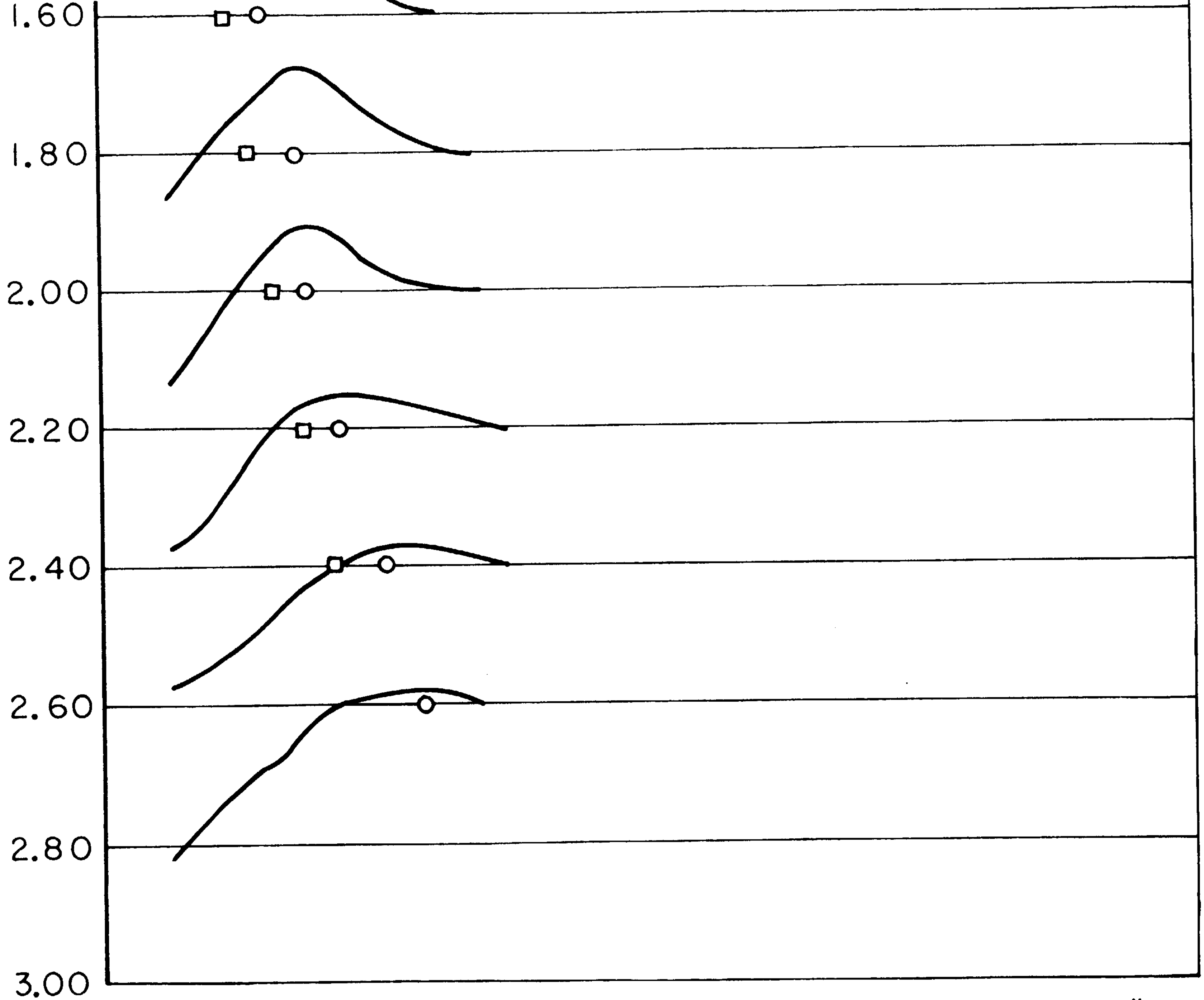

CURRENT DENSITY vs RADIUS FOR 480 μ ARGON IN 8" CHAMBER WITH B-80 PROBE

FIGURE 29

AP25-JPR4030-65

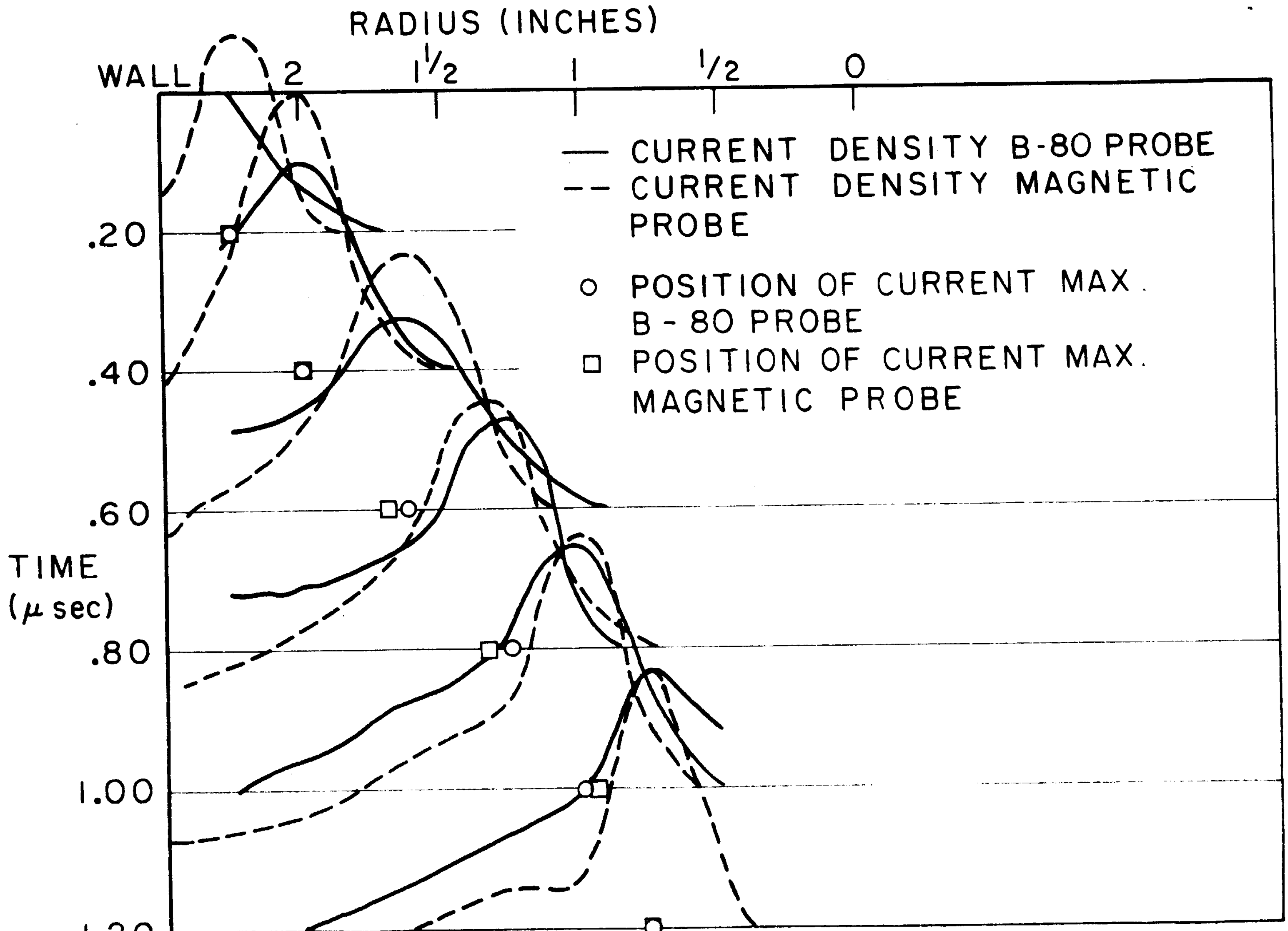

FIGURE

VIII. CONCLUSION AND ACKNOWLEDGEMENTS

Miniature Rogowski coil probes have been shown to measure current density distributions in large-radius pinch discharges with significant savings in data reduction over the more commonly used B probe surveys. Although the original goal of this investigation was to produce an instrument which would produce only qualitative data, semi-quantitative data appears to be attainable, subject to the limitations previously discussed on the design and construction of the probe.

The author very gratefully acknowledges the assistance of Professor Robert G. Jahn who proposed the original concept and who in turn received the idea from M. Begun of Republic Aviation Corporation; Woldemar von Jaskowsky, Rodney Burton, and Neville Black, all of whom were of invaluable aid at various times during the project; and Albert Casini for his untiring assistance in the laboratory.

REFERENCES

1. Glasstone, Samuel and Lovberg, Ralph: "Controlled Thermonculear Reactions," D. Van Nostrand Co., 1960, p. 165.
2. Rose, David J. and Clark, Melville, Jr.: "Plasmas and Controlled Fusion," M.I.T. Press, J. Wiley, 1961, p. 360.
3. Jahn, Robert G. and von Jaskowsky, Woldemar: "Structure of a Large-Radius Pinch Discharge," AIAA Journal 1, 1809 (August 1963).
4. Jahn, Robert G. and von Jaskowsky, Woldemar: "Current Distribution in Large-Radius Pinch Discharges," AIAA Journal 2, 1749 (October 1964).
5. Koeppendorfer, W.: "Induction Coils as Detectors for Fast High Current Gas Discharges," (translation) Institute for Plasma Physics, Munich-Garching, 1961.
6. Butt, E. P. and Gillespie, A. B.: "The Measurement of Voltage, Current, and Magnetic Field in Pulsed Toroidal Gas Apparatus at Harnwell," Volume 2, Instruments and Measurements, Academic Press, 1961, p. 938.